Separation and Purification Technology 241 (2020) 116644

Contents lists available at ScienceDirect

Separation and Purification Technology

journal homepage: www.elsevier.com/locate/seppur

Mechanisms of arsenate removal and membrane fouling in ferric based coprecipitation–low pressure membrane filtration systems

Arslan Ahmad[a,b,c,d,*], Sam Rutten[c], Luuk de Waal[a], Peter Vollaard[d], Case van Genuchten[e,f], Harry Bruning[d], Emile Cornelissen[a], Albert van der Wal[c,d]

[a] KWR Water Cycle Research Institute, Nieuwegein, the Netherlands
[b] KTH-International Groundwater Arsenic Research Group, Department of Sustainable Development, Environmental Science and Engineering, KTH Royal Institute of Technology, Stockholm, Sweden
[c] Department of Environmental Technology, Wageningen University and Research (WUR), Wageningen, the Netherlands
[d] Evides Water Company N.V. Rotterdam, the Netherlands
[e] Geological Survey of Denmark and Greenland (GEUS), Copenhagen, Denmark
[f] Department of Earth Sciences-Geochemistry, Faculty of Geosciences, Utrecht University, Utrecht, the Netherlands

ARTICLE INFO

Keywords:
Arsenic removal
Coprecipitation
Iron chloride
Groundwater treatment
Ultrafiltration
Microfiltration

ABSTRACT

Ferric based coprecipitation–low pressure membrane filtration is a promising arsenic (As) removal method, however, membrane fouling mechanisms are not fully understood. In this study we investigated the effect of feed water composition and membrane pore size on arsenate [As(V)] removal and membrane fouling. We observed that As removal efficiency was independent of the membrane pore size because the size of the Fe(III) particles was larger than the pore size of the membranes, attributed to a high calcium concentration in the feed water. Arsenic coprecipitation with Fe(III) (oxyhydr)oxides rapidly reached equilibrium before membrane filtration, within 1 min. Therefore, As removal efficiency was not improved by increasing residence time before membrane filtration. The removal of As(V) was strongly dependent on feed water composition. A higher Fe(III) dose was required to reduce As(V) to sub-µg/L levels for feed water containing higher concentration of oxyanions such as phosphate and silicate, and lower concentration of cations such as calcium. Cake-layer formation was observed to be the predominant membrane fouling mechanism.

1. Introduction

Arsenic (As) is a well-known human carcinogen, classified in Group 1 by International Agency for Research on Cancer – IARC [12,22,36]. The WHO guideline for As in drinking water is 10 µg/L, however concerns are growing that chronic ingestion of low As concentrations can also adversely affect human health [1,32]. Therefore, certain water treatment companies aim to produce drinking water with As concentrations below 1 µg/L [1,5,38].

Coprecipitation of arsenate [As(V)] with Fe(III) (oxyhydr)oxides is a widely used As removal method [10,14,20,29,34]. For arsenite [As (III)], coprecipitation with Fe(III) (oxyhydr)oxides is less effective in the pH range of most groundwaters because As(III) is uncharged and have a significantly lower affinity for adsorption to Fe(III) (oxyhydr) oxide surfaces. Typically, a Fe(III) coagulant is dosed in water to produce Fe(III) (oxyhydr)oxides which adsorb As(V) from water [20,29]. The As(V) bearing Fe(III) precipitates are subsequently removed in a granular media filter [16,17,19,26,31]. These precipitates can also be removed by low-pressure membranes like microfiltration (MF) and ultrafiltration (UF), especially when removal of colloidal As bearing Fe (III) particles is to be achieved [7,9,15,23,31,42]. However, wide-scale application of low-pressure membrane filtration for As removal is restricted, because of lack of detailed knowledge about membrane fouling due to Fe(III) particles and operational consequences.

Arsenate coprecipitation efficiency with Fe(III) (oxyhydr)oxides and the size of resulting Fe(III) particles is dependent on the ionic composition of water [33,41]. An overview of possible fouling mechanisms for low pressure membranes is presented in Fig. 1. It is expected that the Fe (III) particles which are larger than the membrane pores will be deposited on the membrane surface, i.e. form a cake-layer (Fig. 1A) whereas Fe(III) particles smaller or comparable to the membrane pores will penetrate deeper into membrane structure and cause internal particle deposition (Fig. 1B). Also, fouling can occur due to adhesion of Fe(III) particles to the membrane material (Fig. 1C). To what extent

* Corresponding author at: KWR Water Cycle Research Institute, Groningenhaven 7, 3433 PE Nieuwegein, the Netherlands.
E-mail addresses: arslan.ahmad@kwrwater.nl, arslana@kth.se (A. Ahmad).

https://doi.org/10.1016/j.seppur.2020.116644
Received 9 November 2019; Received in revised form 22 January 2020; Accepted 28 January 2020
Available online 01 February 2020

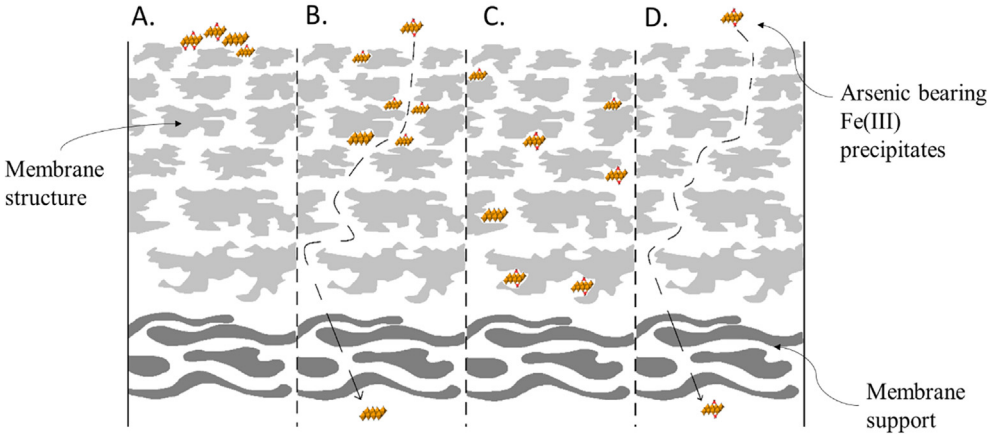

Fig. 1. Different removal mechanisms for As bearing Fe(III) particles expected for low-pressure membrane filtration. (A) Pore size smaller than Fe(III) particles results in cake layer formation and pore blocking (B) Pore size larger or comparable to Fe(III) particles results in internal deposition. (C) Pore size larger than Fe(III) particles and adsorption affinity resulting in internal membrane fouling. (D) Pore size larger than Fe(III) particles without adsorption affinity resulting in transport of particles through the membrane.

these different Fe(III) deposits are removed by backwashing is not yet fully understood. This understanding is required to develop advanced membrane cleaning strategies for sustainable membrane operation.

We have previously shown that As levels much lower than 1 μg/L can be achieved by oxidizing As(III), the predominant As species in anoxic groundwater, by potassium permanganate ($KMnO_4$) before co-precipitation with Fe(III)(oxyhydr)oxides [2]. The use of $KMnO_4$, however, can be avoided by treating the effluents of rapid sand filters (RSFs) which predominantly contain As(V) due to complete As(III) oxidation to As(V) in rapid sand filters (Fig. S1) [2,16,17]. Consequently, the aim of this study is to investigate As(V) removal efficiency and membrane fouling mechanisms during Fe(III) based coprecipitation in combination with low-pressure membrane filtration with the objective to achieve an As reduction to below 1 μg/L in RSF effluents.

2. Materials and methods

2.1. Feed water

Ionic composition of water affects both As(V) adsorption and size of Fe(III) particles [4]. Also the size of Fe(III) particles is expected to impact membrane fouling (Fig. 1). Therefore, we used rapid sand filter effluent samples from two different water treatment plants in the Netherlands (Fig. S2) which are significantly different in ionic composition (Table 1 and Table S1).

2.2. Membrane and module characteristics

To investigate the effect of membrane pore size on As removal and membrane fouling, two commercially available hollow fiber membranes (Pentair X-Flow, The Netherlands) were used which had different average pore sizes (MF: 200 nm and UF: 20 nm, Table 2). Both types of membranes were made of a similar polymeric polyethersulfone and polyvinylpyrrolidone (PES/PVP) material. Also, both membranes were operated inside-out. Fig. 2 presents the scanning electron microscope (SEM) images of the inner-surface and the cross-section of the membranes.

Table 1
Composition rapid sand filter effluent samples, designated as feed 1 and feed 2, obtained from two water treatment plants in the Netherlands.

Parameter	Unit	Feed 1	Feed 2
pH	–	7.8	8.2
Arsenic	μg/L As	2.3	3.3
Iron	μg/L Fe	< 10	< 10
Manganese	μg/L Mn	< 10	< 10
Ortho-phosphate	μg/L P	8	62
Silicate	μg/L Si	3640	4585
Dissolved organic carbon	mg/L C	1.9	2.1
Calcium	mg/L Ca	90	48
Magnesium	mg/L Mg	11	8.5

Table 2
Membrane and module characteristics. Membranes were supplied by Pentair X-Flow, the Netherlands. Modules were constructed at KWR Water Cycle Research Institute, the Netherlands.

	UF membrane	MF membrane
Commercial identification	UFC M5	MF02 M2
Membrane process	Ultrafiltration	Microfiltration
Membrane material	PES/PVP	PES/PVP
Pore size [nm]	20	200
Filtration area [cm^2]	20	20
No. of fibers per module [–]	4	2
Inner fiber diameter [mm]	0.8	1.5
Volume/Area ratio [mm]	0.2	0.4

Experiments were performed with laboratory scale membrane modules that were made by potting (with an epoxy resin) multiple hollow fibre membranes in a transparent polyvinyl chloride (PVC) tube, as previously described by Floris et al. [13]. The total filtration area for both membranes was 20 cm^2, which was realized by installing 2 and 4 hollow fibre membranes for MF and UF respectively.

2.3. Membrane filtration apparatus and filtration procedure

An automated laboratory scale set-up was used for the experiments (Fig. 3). The setup consisted of a pulsation-free neMYSIS syringe pump (Cetoni GmbG, Germany) that supplied feed solution to the membrane module at a constant flow of 8.3 mL/min (corresponding to the flux of 250 L/m^2.h). A membrane pump (ProMinent GmbH, Heidelberg, Germany) was used for in-line dosing of the $FeCl_3$ stock solution in the feed at a constant flow of 0.3 mL/min. The concentration of the $FeCl_3$ stock solution was adjusted to change Fe(III) dose in different experiments. The hydraulic residence time (HRT) between the point of Fe(III) dose and membrane filtration was 1 min in all the experiments except for the study of coprecipitation kinetics where a HRT of 5 min was applied. The increased HRT before membrane filtration was achieved by increasing the length of the feed tube. The *trans*-membrane pressure (TMP) was measured by a sensor (Wika Transmitter 891.13.500) every second and logged using SquirrelView Data Logger (Grant Instruments, Cambridge, UK).

Each experiment consisted of 6 consecutive filtration (1 h each) and backwash cycles (33.3 mL/min, 20 sec each cycle). Ultrapure water was used for backwashing and the backwash flow was provided by a pressurised vessel (3 bars) combined with an adjustable flow control. Samples of the feed water, including Fe(III) dosing, were collected directly by opening the valve (point 2 in Fig. 3). Permeate was sampled

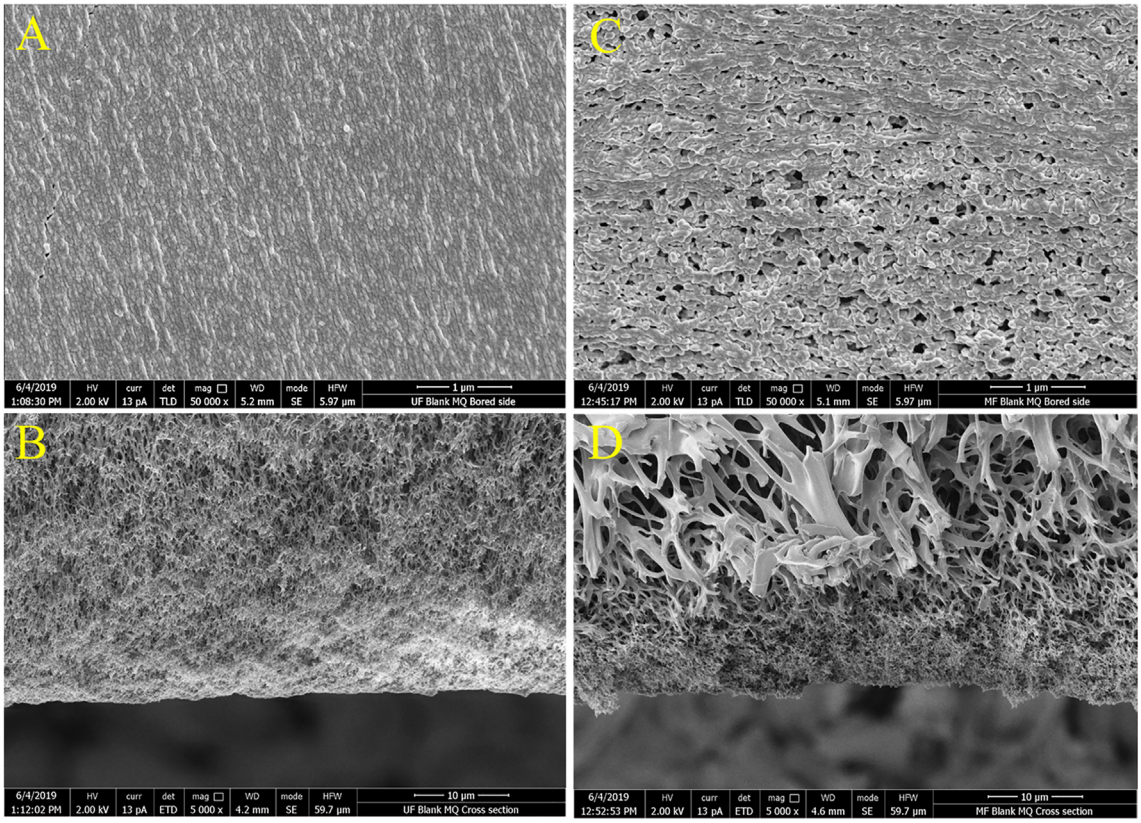

Fig. 2. The SEM micrographs of the UF and MF membranes. The membranes were pre-conditioned with ultrapure water. (A) and (C) show the inner-surface of the UF and MF respectively and (B) and (D) show the cross-section of the UF and MF respectively.

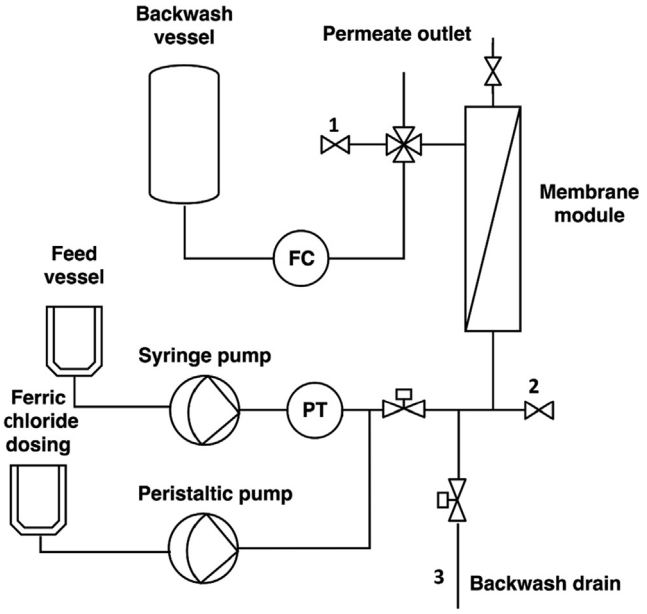

Fig. 3. Schematic diagram of the experimental setup. Points marked as 1, 2 and 3 indicate permeate, feed and backwash water sampling points, respectively.

from a beaker that collected the entire permeate volume produced during a filtration cycle (point 1 in Fig. 3), except in the experiments where the effect of successive filtration cycles on As(V) removal was studied. Backwash samples were collected from a beaker that collected the entire backwash water volume produced during a backwash cycle (point 3 in Fig. 3).

2.4. Reagents and chemicals

Ferric chloride was dosed using a stock solution that was prepared by dissolving $FeCl_3{\cdot}6H_2O$ (CAS: 10025–77-1, 97% purity, J.T Baker, Deventer, the Netherlands) in 0.5 L ultrapure water. A stock solution of 1.0 g/L As_2O_5 (CAS: 12044–50-7, 99% purity) obtained from inorganic ventures (Nieuwegein, the Netherlands) was used to spike the water with As(V). The ultrapure water was obtained by treating distilled water with a Purelab Chorus (Veolia, the Netherlands).

2.5. Analysis methods for water samples

Arsenic, Fe, Ca, Mg, Si, P were measured by inductively coupled plasma mass spectrometry (ICP-MS) using the Thermo Scientific iCAP TQ (Thermo Fisher Scientific, Breda, the Netherlands). Total organic carbon analysis was carried out with a Shimadzu TOC-V_{CPH} total organic carbon analyser (Shimadzu Benelux, 's-Hertogenbosch, the Netherlands).

2.6. SEM-EDX analysis

Samples of the fouled UF membranes (membrane after 6 filtration and 5 backwash cycles) and backwashed membranes (6 filtration and 6 backwash cycles) were analyzed by SEM to gain further insights into fouling mechanisms. The analysis was carried out at the Wageningen Electron Microscopy Centre at Wageningen University (WUR), using a SEM device (FEI Magellan 400) that was equipped with an Oxford Instruments X-MAX X-ray detector for energy dispersive X-ray (EDX) analysis. The virgin MF and UF membranes were conditioned by ultrapure water passage before the SEM analysis. For analysis of each sample, two fragments of the bore side (longitudinal cut) and two fragments of the cross-section (transversal cut) were fixed on a sample holder and coated with tungsten using a Leica SCD 500 sputtercoater.

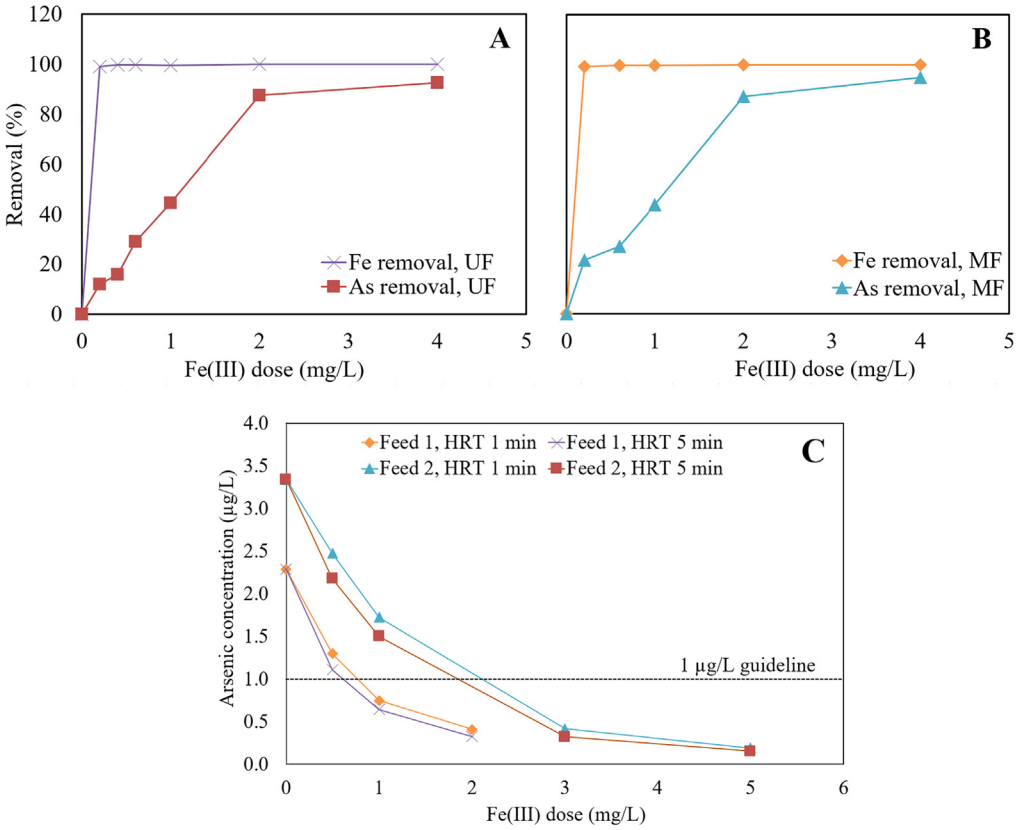

Fig. 4. Removal efficiency of As and Fe in function of Fe(III) dose in experiments with (A) UF and (B) MF. The experiments were performed with Feed 1 after spiking with As(V) to achieve initial As = As (V) = 5 µg/L. The removal of 80% corresponds to 1 µg/L residual As in water. (C) Residual As in function of Fe(III) dose, feed water quality and hydraulic residence time between point of Fe(III) dosing and UF. Feed 1 and Feed 2 were not spiked with additional As(V).

2.7. Calculations

2.7.1. Rejection efficiency

The rejection efficiency of a solute (e.g. As and Fe) during filtration is given by

$$R_i = \left(1 - \frac{C_p}{C_f}\right)_i \times 100[\%] \quad (1)$$

where R_i is the rejection efficiency of a solute i, C_p is the permeate concentration and C_f is the feed concentration (mg/L).

2.7.2. Membrane permeability recovery

To assess the retention mechanism of Fe(III) particles, the evolution of membrane permeability under different conditions was analyzed. The membrane permeability was calculated according to

$$k = \frac{J}{TMP}[\mathrm{L/m^2{\cdot}h{\cdot}bar}] \quad (2)$$

where k is the membrane permeability, J is the flux (L/m^2.h) and TMP is the *trans*-membrane pressure (bar).

The permeability recovery for each backwash cycle was calculated by

$$k_R = \frac{k_{after\ \ backwash}}{k_{clean\ \ membrane}} \times 100[\%] \quad (3)$$

where k_R is the permeability recovery, $k_{after\ backwash}$ is the membrane permeability after backwash and $k_{clean\ membrane}$ is the permeability of the virgin membrane.

2.7.3. Fouling analysis with resistance-in-series model

To assess the predominant membrane fouling mechanisms, we developed a resistance in series model [6,13,27].

For the flux in porous media we use Darcy's Law [8,28] which is given by

$$J = TMP/(\nu{\cdot}R_T)[\mathrm{L/m^2{\cdot}h}] \quad (4)$$

where ν is the dynamic viscosity of the solution (Pa.s) and R_T is the total resistance to filtration (1/m) which is the sum of clean membrane resistance (R_M), resistance due to the external cake-layer deposition (R_E) and the resistance due to the internal deposition (R_I).

$$R_T = R_M + R_E + R_I[1/\mathrm{m}] \quad (5)$$

We obtain R_M by filtration of ultrapure water through a virgin membrane according to Eq. (4) and is given by

$$R_M = \left(\frac{TMP}{\nu{\cdot}J}\right)_{virgin,ultrapurewater}$$

The filtration of feed water, which includes Fe(III) particles, through a virgin membrane is expected to cause membrane fouling due to particle deposition and therefore R_T can be obtained as follows.

$$R_T = \left(\frac{TMP}{\nu{\cdot}J}\right)_{fouled}$$

The internal and external fouling resistance ($R_E + R_I$) is equal to R_T–R_M.

We further assume that the hydraulic backwash will remove all the external fouling (we checked this assumption by SEM–EDX, see Section 3.2.2). We therefore obtain R_I as follows

$$R_I = \left(\frac{TMP}{\nu{\cdot}J}\right)_{backwashed}$$

We finally determine R_E by subtracting the membrane resistance (R_M) and internal resistance (R_I) from the total resistance (R_T).

3. Results and discussion

3.1. Arsenic removal efficiency

3.1.1. Impact of membrane pore size

The effect of membrane pore size on As(V) removal efficiency was studied using Feed 1 which had been spiked to achieve 5 µg/L As(V) concentration. The experiments included dosing of different Fe(III) concentrations (0–4 mg/L) into the feed solution and filtration-backwash cycles. We observed that in the absence of Fe(III) dose, no As(V) was removed for both MF and UF membranes (Fig. 4A and 4B) due to the small size of As(V) oxyanion [3,25]. Also, adsorption of As(V) to the membranes did not occur because of lack of affinity between As(V) oxyanion (Fig. S3) and the membranes which have been shown to have a negative surface charge in previous studies [13,24,37]. With Fe(III) dosing, As(V) removal was significant, due to coprecipitation of As(V) with formed Fe(III) (oxyhydr)oxides [15]. Arsenic removal efficiency increased with increasing Fe(III) dosage for both MF and UF membranes. Also, the removal of Fe close to 100% was observed in all cases (Fig. 4A and B). These results indicate that As removal efficiency was independent of membrane pore sizes because the size of Fe(III) particles was larger than, or at least comparable to, the membrane pore sizes. This conclusion is also supported by Ahmad et al. [4] where we observed Fe(III) particle sizes in the range of 2–80 µm (25 µm most abundant). The growth of Fe(III) precipitates to such large sizes can be attributed to the natural presence of high Ca concentrations in given feed water [4].

3.1.2. Impact of feed water composition and hydraulic residence time

Arsenic coprecipitation with Fe(III) (oxyhydr)oxides is known to be sensitive to ionic composition of water [4,29,40]. To gain further insights into the effect of water composition on As removal, experiments were carried out with the two feed solutions with different ionic composition using UF membranes. Arsenic concentrations below 1 µg/L were obtained by dosing 1 mg/L Fe(III) dose for Feed 1 and 3 mg/L Fe (III) dose for Feed 2 (Fig. 4C). The lower As(V) removal efficiency for Feed 1 compared to Feed 2 can be explained by taking into account the effect of feed water composition on the coprecipitation of As(V) and Fe (III) (oxyhydr)oxides. For example, the concentration of phosphate and silicate oxyanions, which compete with As(V) for adsorption sites on Fe (III) (oxyhydr)oxides, is much higher in Feed 2 than Feed 1 (Table 1). In addition, Feed 2 has a lower concentration of bivalent cations than Feed 1 (90 mg/L compared to 48 mg/L Ca). It is known that the presence of bivalent cations can enhance the efficiency of As(V) coprecipitation with Fe(III) (oxyhydr)oxides involving mechanisms such as neutralization of the Fe(III) precipitate surface charge by Ca and formation of ternary complexes between Fe(III), As(V) and Ca [39,40,41]. Finally, Feed 1 has a lower pH compared to Feed 2 which can also contribute to the higher As adsorption to Fe(III) precipitates due to the fact that Fe (III) (oxyhydr)oxides at lower pH will have more positive charge on the surface and hence a higher number of adsorption sites for oxyanions [21,30].

To gain insights into the kinetics of As(V) and Fe(III) (oxyhydr)oxide coprecipitation, a set of experiments was carried out at an increased HRT of 5 min before removal of the formed Fe(III) (oxyhydr)oxides by the membranes. Results show that As(V) concentrations in the permeate at 5 min HRT is comparable to As(V) concentrations found in experiments having 1 min HRT (applied in all experiments) (Fig. 4C), indicating that As(V) coprecipitation with Fe(III) (oxyhydr)oxides rapidly reached equilibrium within 1 min. Such rapid coprecipitation of As has also been reported in previous studies [14,18,30].

We also studied As(V) removal as a function of the successive number of filtration cycles (filtration cycles 1, 3 and 6). No differences were observed for As(V) removal between the filtration cycles (Fig. 5), confirming that As(V) uptake by Fe(III) precipitates reached equilibrium before the suspension entered the membrane, i.e. in 1 min.

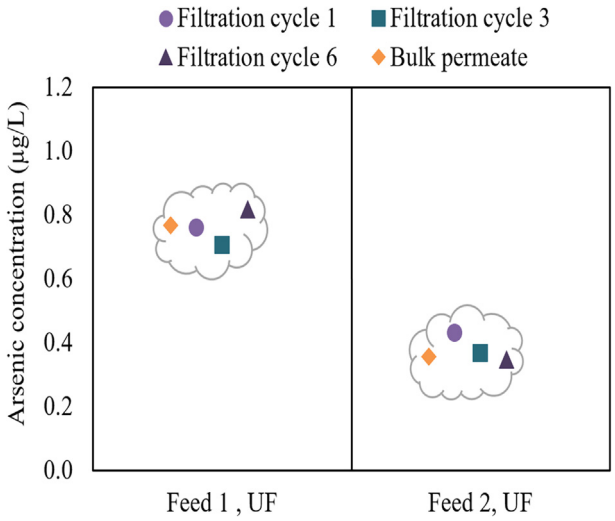

Fig. 5. Arsenic removal in function of the number of filtration cycles. Only UF membranes were used for this experiment. Fe(III) dose for Feed 1 and Feed 2 was 1 mg/L and 3 mg/L, respectively. Bulk permeate refers to total permeate volume produced by the 6 filtration cycles.

Table 3
Clean water permeability and corresponding resistance calculated from the ultrapure water flux.

	UF	MF*
Permeability (L/m^2.hour.bar)	(1.25 ± 0.08) × 10^3	> 3.13 × 10^5
Membrane resistance (1/m)	(2.88 ± 0.24) × 10^{11}	< 1.15 × 10^9

* TMP was lower than the lower measurement limit of the sensor (0.0008 bar).

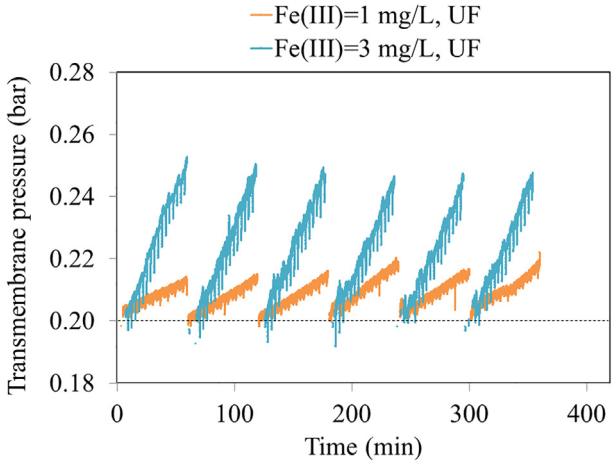

Fig. 6. Evolution of TMP during UF experiments. During the experiments, flux was constant at 250 L/m^2.h. For MF the TMP was consistently lower than the lower measurement limit (0.0008 bar) therefore not shown in the graph.

3.2. Membrane fouling

3.2.1. Clean water flux measurements

Prior to dosing Fe(III), the membranes were conditioned using ultrapure water at a flux of 250 L/m^2 h until a stable TMP was achieved (normally 1 h). The calculated permeability (k) and the membrane resistance (R_M) (Table 3) were used for the permeability recovery calculations (following sections) and to verify the integrity of the membrane modules before each experiment. The TMP for MF was lower than the measurement limit of the sensor in the experimental setup

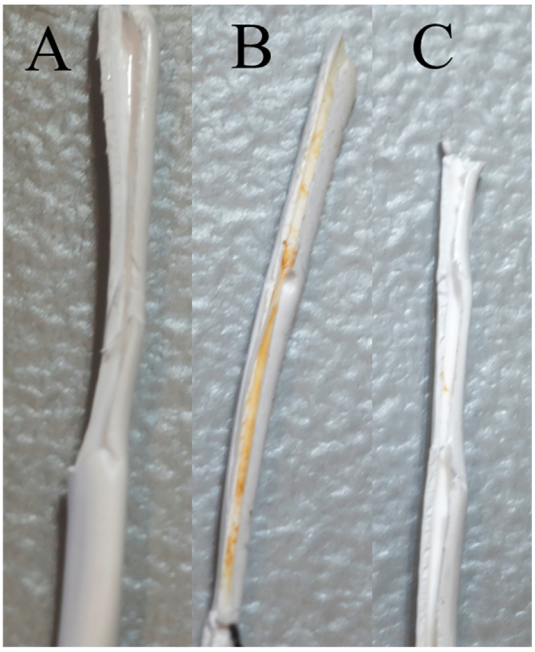

Fig. 7. The visuals of the UF membranes after experiments with Feed 2 dosed with 3 mg/L Fe(III). (A) Virgin membrane after conditioning with ultrapure water, (B) UF before backwash (membrane after 6 filtration and 5 backwash cycles) and (C) UF after backwash (6 filtration and 6 backwash cycles).

(0.0008 bar) and therefore the exact permeability could not be calculated for MF. In the following sections we discuss Fe(III) particle retention and fouling of UF membranes.

3.2.2. Fouling of UF membranes

Fig. 6 presents the effect of Fe(III) particle deposition on TMP during 6 filtration–backwash cycles for Feed 1 and Feed 2 with 1 and 3 mg/L Fe(III) dosing respectively which resulted in As below 1 µg/L in the permeate. The initial TMP (clean membrane) was similar for both feeds, but the difference in Fe(III) dose produced clear differences in TMP increase during the filtration cycles. For example, the average TMP increase per cycle for Feed 1 and Feed 2 was 0.012 and 0.072 bar/h respectively which shows the higher susceptibility of membrane fouling at a higher Fe(III) dose. Nevertheless, in both cases the initial TMP was effectively restored after the backwash procedure (Fig. 6 and Fig. S4), indicating a predominance of reversible fouling at 1 and 3 mg/L Fe(III) dosing.

To further elucidate fouling mechanisms, membranes were analyzed visually and with SEM–EDX (Figs. 7–9). The visual effect of the deposition of Fe(III) precipitates on UF membrane before backwash (i.e. after 6 filtration and 5 backwash cycles) compared to after backwash (i.e. 6 filtration and 6 backwash cycles) in an experiment with Feed 2 dosed with 3 mg/L Fe(III) (As below 1 µg/L) is presented in Fig. 7. The surface of the UF before backwash is visually very different from both the virgin UF membrane and the backwashed UF membrane. It shows an irregular layer of reddish-brown deposit (As bearing Fe(III) precipitates). No such deposits are observed in the virgin and backwashed UF membranes which implies that the hydraulic backwash effectively

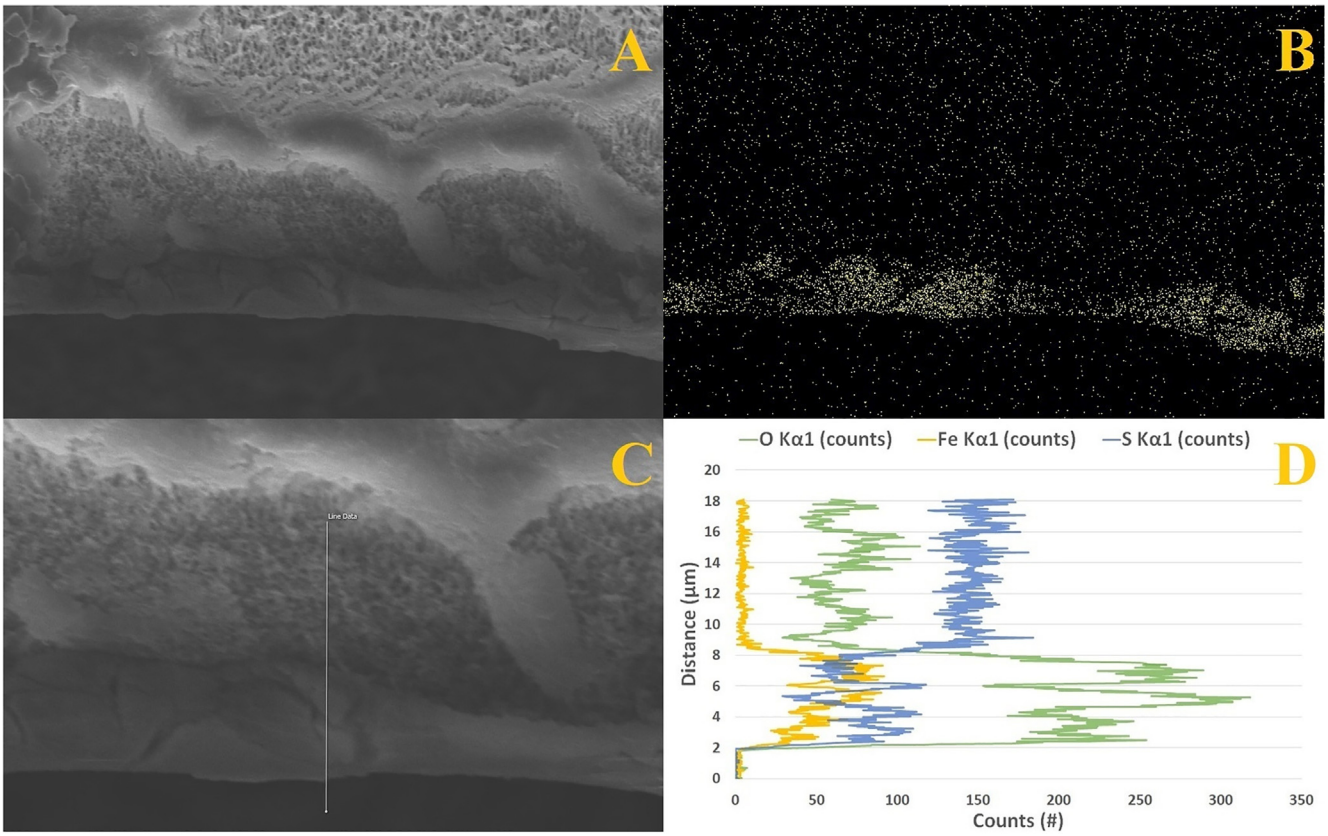

Fig. 8. SEM micrograph (A and C) and EDX scans (B and D) of the cross section of the UF membrane specimen shown in Fig. 7B. (A) Cross section of UF membrane before backwash. (B) EDX spectrum of Fig. 8A, showing signal from Fe-atoms, indicating the presence of a Fe-based cake layer on the membrane surface. (C) Enlarged section of Fig. 8A, indicating the line at which EDX data is acquired. (D) EDX data of the line in Fig. 8C, highlighting Fe (yellow), O (green) and S (blue) signals along the line as function of detector-counts per second (cps). The dot on the line in Fig. 8C equals 0 µm on the y-axis of Fig. 8D. At distance > 8 µm, increasing sulfur signal indicates the presence of the supporting layer. At distance 8–2 µm, low sulfur signal and higher iron and oxygen signal indicates the presence (and thickness) of the deposited Fe(III) (oxyhydr)oxide cake-layer. For interpretation of the references to colour in this figure legend, the reader is referred to the web version of this article.

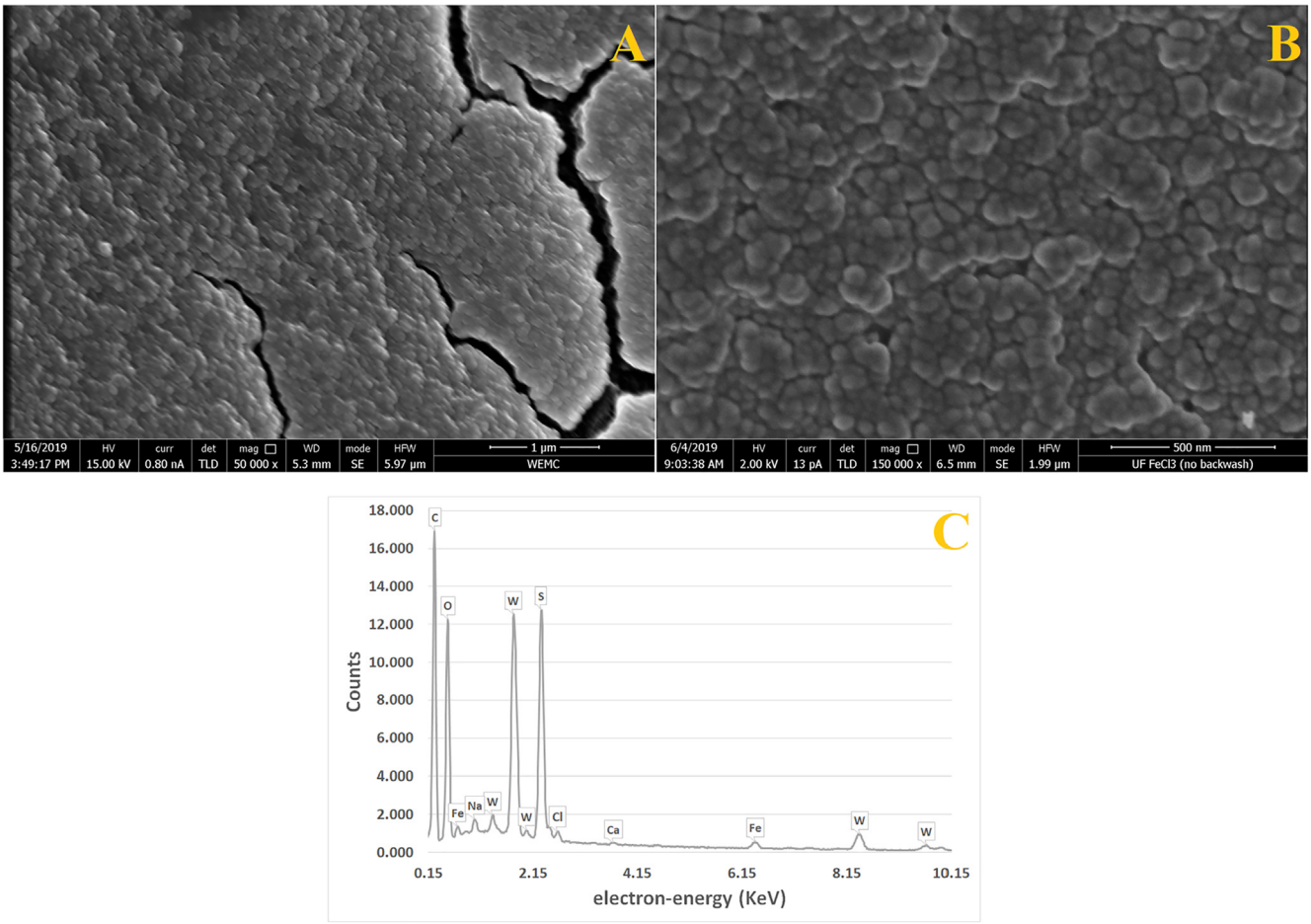

Fig. 9. SEM–EDX of the solid depositions found on the bored side of the UF membrane. (A) 50 000× maginified image (B) 150 000× magnified image. (C) Spectrum shows the elemental composition at the bored side of the UF before backwash. Na and Cl are present due to the drying and crystallization of NaCl. The small calcium peak can be explained by coprecipitation of calcium with Fe(III)(oxyhydr)oxides. The high carbon, oxygen and sulfur peaks are from the membrane material (PES, $(C_{12}H_8O_3S)_n$). Tungsten was used to coat the sample. The observed fractures in the cake layer in Fig. 9A is an artefact and caused by drying during preparation or storage. The deposits in Fig. 9B appear to consist of primary spherical particles with an average size 65 nm.

removed the Fe(III) deposits.

SEM micrographs and EDX scans of the cross section of the fouled UF membrane (i.e. the membrane specimen shown in Fig. 7B), show Fe-signal restricted only to an approximate depth of 7 µm on the membrane surface (Fig. 8). This confirms that Fe(III) particles were deposited as a cake-layer on membrane surface. Thus, based on membrane permeability recovery and complimentary visual and SEM-EDX analysis we conclude that the removal of As bearing Fe(III) particles occurred largely on the surface of UF membrane i.e. by cake-layer formation. Membrane permeability was reduced during a filtration cycle probably due to a growing cake on the membrane surface and a hydraulic backwash effectively removed the surface deposits and restored membrane permeability (Fig. 6 and Fig. S4).

3.2.3. Fouling analysis by resistance-in-series model

The resistance model (see Section 2.7.3) was used to further understand the fouling and contribution of different resistances during filtration. For both Feed 1 and Feed 2, dosed with different Fe(III) concentrations, the total resistance was dominated by membrane resistance (R_M) followed by external resistance (R_E) (Fig. 10A). The internal resistance (R_I), on the other hand, was very small and may be due to some internal deposition of Fe(III) particles which might have penetrated somewhat deeper into the membrane pores [35]. Particles deposited within the membrane pore structure are likely to be subjected to lower hydraulic shear forces and are therefore not effectively removed by hydraulic backwashing [11]. The contribution of R_E for Feed 2 was higher than Feed 1 which can be explained easily by the higher Fe(III) dose applied for Feed 2.

The resistance analysis was also carried out with different Fe(III) doses in Feed 1 (Fig. 10B). The total resistance systematically increased with the increments in Fe(III) dose. Again, R_M dominated the total resistance followed by R_E and the R_I was the smallest. The systematic increase in the R_E as a function of Fe(III) dose is consistent with the trend observed (cake-layer build-up) in the experiments with Feed 1 and Feed 2 at their specific optimum Fe(III) doses required for As removal to below 1 µg/L (Fig. 10A). Thus, cake-layer formation was found to be the major proportion of fouling resistance.

4. Conclusions and implications for the practice

The removal of As(V) and membrane fouling mechanisms during Fe(III) based coprecipitation–low pressure membrane filtration were studied for achieving As reduction to very low levels below 1 µg/L in rapid sand filter effluents. We found that As(V) removal efficiency was independent of the membrane pore size because the size of the Fe(III) particles was larger than the pore size of UF and MF membranes. Also, As(V) coprecipitation with Fe(III) (oxyhydr)oxides rapidly reached equilibrium before membrane filtration, within 1 min. This resulted in a stable As removal efficiency even at an increased residence time of 5 min before membrane filtration. The removal efficiency of As(V) was nevertheless dependent on feed water composition, in such a way that a higher Fe(III) dose was required to reduce As to below 1 µg/L for the

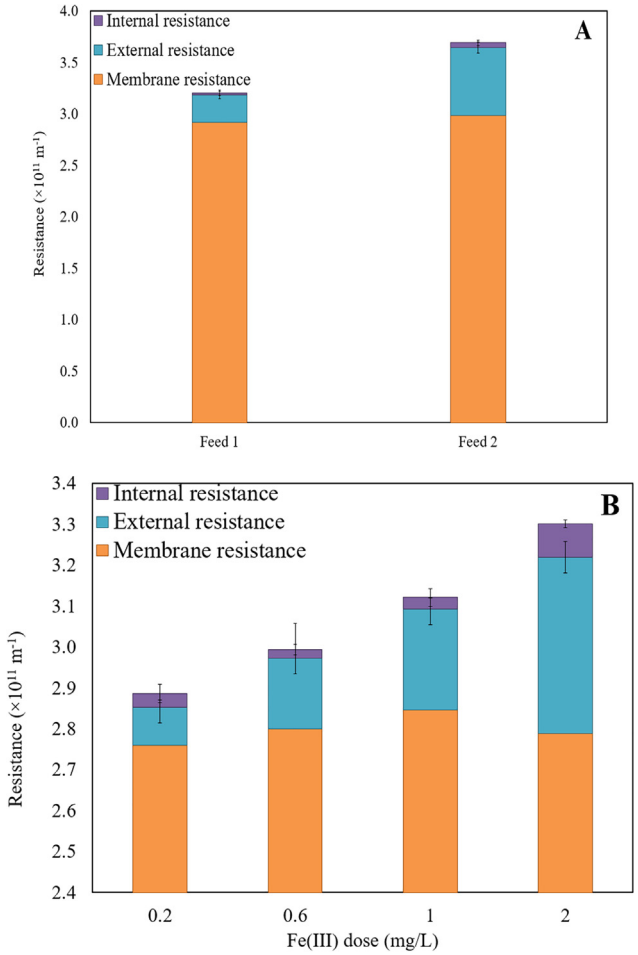

Fig. 10. Resistance model analysis for the UF experiments for (A) Feed 1 which was dosed with 1 mg/L Fe(III) and Feed 2 which was dosed with 3 mg/L Fe(III) and (B) Feed 1 which was dosed with different Fe(III) doses (0.2–2 mg/L).

feed water which had higher phosphate and silicate concentrations and lower calcium and magnesium concentrations.

In all the UF experiments, Fe(III) particles formed a cake-layer on the membrane surface which reduced membrane permeability during filtration. The cake on the UF membranes was effectively removed with a hydraulic backwash, resulting in near-complete restoration of membrane permeability. The fouling mechanisms for MF, on the other hand, could not be studied in detail and therefore it is difficult to draw clear conclusions about MF fouling. However, we postulate for future work that more open low-pressure membranes may be more susceptible to irreversible fouling due to a large pore size which can allow some Fe (III) particles to penetrate deeper into the membrane structure and get immobilized there.

It is noteworthy that direct translation of our results for long-term application may be limited by the fact that we studied the membrane fouling only for 6 filtration and backwash cycles. At water treatment plants, long term membrane operation can result in a significant permeability reduction due to slow build-up of internal membrane fouling which was negligibly small in our UF experiments.

CRediT authorship contribution statement

Arslan Ahmad: Conceptualization, formal analysis, writing-original draft, project administration. **Sam Rutten:** Data curation, investigation. **Luuk de Waal:** Data curation, investigation. **Peter Vollaard:** Data curation, investigation. **Case van Genuchten:** Writing - review & editing. **Harry Bruning:** Conceptualization, supervision. **Emile Cornelissen:** Conceptualization, supervision, writing-review & editing. **Albert van der Wal:** Funding acquisition, Supervision, writing-review & editing.

Declaration of Competing Interest

The authors declare that they have no known competing financial interests or personal relationships that could have appeared to influence the work reported in this paper.

Acknowledgement

This research is co-financed with PPS-funding from the Topconsortia for Knowledge & Innovation (TKI) of the Ministry of Economic Affairs and Climate. AA acknowledges support from Evides Waterbedrijf. We thank Marcel Giesbers and Jelmer Vroom at Wageningen Electron Microscopy Centre for assistance during SEM data collection.

Appendix A. Supplementary material

Supplementary data to this article can be found online at https://doi.org/10.1016/j.seppur.2020.116644.

References

[1] A. Ahmad, P. Bhattacharya, Arsenic in Drinking Water: Is 10 µg/L a Safe Limit? Current Pollution Reports (2019).
[2] A. Ahmad, E. Cornelissen, S. van de Wetering, T. van Dijk, C. van Genuchten, J. Bundschuh, A. van der Wal, P. Bhattacharya, Arsenite removal in groundwater treatment plants by sequential Permanganate-Ferric treatment, J. Water Process Eng. 26 (2018) 221–229.
[3] Ahmad, A., Richards, L.A., Bhattacharya, P. Arsenic remediation of drinking water: an overview. In Bhattacharya, P., Polya, D.A., Jovanovic, D. (Eds.) Best Practice Guide on the Control of Arsenic in Drinking Water (2017), IWA Publishing UK. p. 79-98. ISBN: 9781780404929.
[4] A. Ahmad, S. Rutten, M. Eikelboom, L. de Waal, H. Bruning, P. Bhattacharya, A. van der Wal, Impact of phosphate, silicate and natural organic matter on the size of Fe (III) precipitates and arsenate co-precipitation efficiency in calcium containing water, Sep. Purif. Technol. (2019).
[5] A. Ahmad, P. Van der Wens, K. Baken, L. De Waal, P. Bhattacharya, P. Stuyfzand, Arsenic reduction to < 1 µg/L in Dutch drinking water, Environ. Int. (2019).
[6] G.D. Bella, D.D. Trapani, A brief review on the resistance-in-series model in membrane bioreactors (MBRs), Membranes 9 (2) (2019) 24.
[7] P. Brandhuber, G. Amy, Alternative methods for membrane filtration of arsenic from drinking water, Desalination 117 (1) (1998) 1–10.
[8] J. Busch, A. Cruse, W. Marquardt, Modeling submerged hollow-fiber membrane filtration for wastewater treatment, J. Membr. Sci. 288 (1) (2007) 94–111.
[9] K.Y.-J. Choi, B.A. Dempsey, In-line coagulation with low-pressure membrane filtration, Water Res. 38 (19) (2004) 4271–4281.
[10] S. Dixit, J.G. Hering, Comparison of arsenic(V) and arsenic(III) sorption onto iron oxide minerals: Implications for arsenic mobility, Environ. Sci. Technol. 37 (18) (2003) 4182–4189.
[11] A.G. Fane, W. Xi, W. Rong, Interface science and technology, Elsevier, 2006, pp. 109–132.
[12] C. Ferreccio, C. González, V. Milosavjlevic, G. Marshall, A.M. Sancha, A.H. Smith, Lung cancer and arsenic concentrations in drinking water in Chile, Epidemiology 11 (6) (2000) 673–679.
[13] R. Floris, K. Nijmeijer, E.R. Cornelissen, Removal of aqueous nC_{60} fullerene from water by low pressure membrane filtration, Water Res. 91 (2016) 115–125.
[14] C.C. Fuller, J.A. Davis, G.A. Waychunas, Surface chemistry of ferrihydrite: Part 2. Kinetics of arsenate adsorption and coprecipitation, Geochim. Cosmochim. Acta 57 (10) (1993) 2271–2282.
[15] G. Ghurye, D. Clifford, A. Tripp, Iron coagulation and direct microfiltration to remove arsenic from groundwater, Am. Water Works Assoc. 96 (4) (2004) 143–152.
[16] J.C.J. Gude, K. Joris, K. Huysman, L.C. Rietveld, D. van Halem, Effect of supernatant water level on As removal in biological rapid sand filters, Water Res. X 1 (2018) 100013.
[17] J.C.J. Gude, L.C. Rietveld, D. van Halem, Fate of low arsenic concentrations during full-scale aeration and rapid filtration, Water Res. 88 (2016) 566–574.
[18] J.C.J. Gude, L.C. Rietveld, D. van Halem, As(III) oxidation by MnO2 during groundwater treatment, Water Res. 111 (2017) 41–51.
[19] J.C.J. Gude, L.C. Rietveld, D. van Halem, Biological As(III) oxidation in rapid sand filters, J. Water Process Eng. 21 (2018) 107–115.
[20] J.G. Hering, P.-Y. Chen, J.A. Wilkie, M. Elimelech, S. Liang, Arsenic removal by ferric chloride, Am. Water Works Assoc. 88 (4) (1996) 155–167.
[21] M. Kanematsu, T.M. Young, K. Fukushi, P.G. Green, J.L. Darby, Arsenic(III, V) adsorption on a goethite-based adsorbent in the presence of major co-existing ions:

Modeling competitive adsorption consistent with spectroscopic and molecular evidence, Geochim. Cosmochim. Acta 106 (2013) 404–428.
[22] S. Kapaj, H. Peterson, K. Liber, P. Bhattacharya, Human health effects from chronic arsenic poisoning–a review, J. Environ. Sci. Health A Tox. Hazard. Subst. Environ. Eng. 41 (10) (2006) 2399–2428.
[23] N. Lee, G. Amy, J.-P. Croué, H. Buisson, Identification and understanding of fouling in low-pressure membrane (MF/UF) filtration by natural organic matter (NOM), Water Res. 38 (20) (2004) 4511–4523.
[24] Sheng Li, S.G.J. Heijman, J.Q.J.C. Verberk, Pierre Le Clech, Jie Lu, A.J.B. Kemperman, G.L. Amy, J.C. van Dijk, Fouling control mechanisms of demineralized water backwash: Reduction of charge screening and calcium bridging effects, Water Res. 45 (19) (2011) 6289–6300, https://doi.org/10.1016/j.watres.2011.08.004.
[25] V.T. Luong, E.E. Cañas Kurz, U. Hellriegel, T.L. Luu, J. Hoinkis, J. Bundschuh, Iron-based subsurface arsenic removal technologies by aeration: A review of the current state and future prospects, Water Res. 133 (2018) 110–122.
[26] L.S. McNeill, M. Edwards, Soluble arsenic removal at water treatment plants, Am. Water Works Assoc. 87 (4) (1995) 105–113.
[27] J. Mulder, Basic principles of membrane technology, Springer Science & Business Media, 2012.
[28] A.N.L. Ng, A.S. Kim, A mini-review of modeling studies on membrane bioreactor (MBR) treatment for municipal wastewaters, Desalination 212 (1) (2007) 261–281.
[29] J. Qiao, Z. Jiang, B. Sun, Y. Sun, Q. Wang, X. Guan, Arsenate and arsenite removal by FeCl3: Effects of pH, As/Fe ratio, initial As concentration and co-existing solutes, Sep. Purif. Technol. 92 (2012) 106–114.
[30] K.P. Raven, A. Jain, R.H. Loeppert, Arsenite and arsenate adsorption on ferrihydrite: kinetics, equilibrium, and adsorption envelopes, Environ. Sci. Technol. 32 (3) (1998) 344–349.
[31] L. Ruiping, S. Lihua, Q. Jiuhui, L. Guibai, Arsenic removal through adsorption, sand filtration and ultrafiltration: In situ precipitated ferric and manganese binary oxides as adsorbents, Desalination 249 (3) (2009) 1233–1237.
[32] N. Saint-Jacques, P. Brown, L. Nauta, J. Boxall, L. Parker, T.J.B. Dummer, Estimating the risk of bladder and kidney cancer from exposure to low-levels of arsenic in drinking water, Nova Scotia, Canada, Environ. Int. 110 (2018) 95–104.
[33] A.C. Senn, S.J. Hug, R. Kaegi, J.G. Hering, A. Voegelin, Arsenate co-precipitation with Fe(II) oxidation products and retention or release during precipitate aging, Water Res. 131 (2018) 334–345.
[34] Q. Shi, C. Jing, X. Meng, Competing interactions of As adsorption and Fe(III) Polymerization during Ferric coprecipitation treatment, Environ. Sci. Technol. 52 (13) (2018) 7343–7350.
[35] X. Shi, G. Tal, N.P. Hankins, V. Gitis, Fouling and cleaning of ultrafiltration membranes: A review, J. Water Process Eng. 1 (2014) 121–138.
[36] C. Steinmaus, Y. Yuan, D. Kalman, O.A. Rey, C.F. Skibola, D. Dauphine, A. Basu, K.E. Porter, A. Hubbard, M.N. Bates, M.T. Smith, A.H. Smith, Individual differences in arsenic metabolism and lung cancer in a case-control study in Cordoba, Argentina, Toxicol. Appl. Pharmacol. 247 (2) (2010) 138–145.
[37] K.W. Trzaskus, A. Zdeb, W.M. de Vos, A. Kemperman, K. Nijmeijer, Fouling behavior during microfiltration of silica nanoparticles and polymeric stabilizers, J. Membr. Sci. 505 (2016) 205–215.
[38] P. Van der Wens, K. Baken, M. Schriks, Arsenic at low concentrations in Dutch drinking water: assessment of removal costs and health benefits, in: P. Bhattacharya, M. Vahter, J. Jarsjö, J. Kumpiene, A. Ahmad, C. Sparrenbom, G. Jacks, M.E. Donselaar, J. Bundschuh, R. Naidu (Eds.), Arsenic at low concentrations in Dutch drinking water: assessment of removal costs and health benefits, CRC Press, Stockholm, Sweden, 2016, pp. 563–564.
[39] C.M. Van Genuchten, A.J. Gadgil, J. Peña, Fe(III) nucleation in the presence of bivalent cations and oxyanions leads to subnanoscale 7 Å polymers, Environ. Sci. Technol. 48 (20) (2014) 11828–11836.
[40] C.M. Van Genuchten, J. Pena, S. Amrose, E. and Gadgil, A.J., Structure of Fe(III) precipitates genberated by the electrolytric dissolution of Fe(0) in the presence of groundwater ions, Geochimica et Cosmochimica Acta, 127 2014, pp. 285–304.
[41] A. Voegelin, R. Kaegi, J. Frommer, D. Vantelon, S.J. Hug, Effect of phosphate, silicate, and Ca on Fe(III)-precipitates formed in aerated Fe(II)- and As(III)-containing water studied by X-ray absorption spectroscopy, Geochim. Cosmochim. Acta 74 (1) (2010) 164–186.
[42] A. Zouboulis, I. Katsoyiannis, Removal of arsenate from contaminated water by coagulation-direct filtration, Sep. Sci. Technol. 37 (12) (2002) 2859–2873.